

The NANOKHOD Microrover – Development of an Engineering Model for Mercury Surface Exploration

André Schiele^{1*}, Jens Romstedt¹, Chris Lee², Hartmut Henkel², Sabine Klinkner², Reinhold Bertrand³, Rudi Rieder^{4#}, Ralf Gellert⁴, Göstar Klingelhöfer⁵, Bodo Bernhardt^{2,5}, Harald Michaelis⁶

¹ESA/ESTEC, Keplerlaan 1, 2200 AG Noordwijk, Netherlands

²von Hoerner & Sulger GmbH, Schlossplatz 8, 68723 Schwetzingen, Germany

³ESA/ESOC, Robert-Bosch-Str. 5, 64293 Darmstadt, Germany

⁴Max-Planck-Institut für Chemie, J.J. Becherweg 27, 55128 Mainz, Germany

⁵Johannes Gutenberg-Universität Mainz, Staudinger Weg 9, 55099 Mainz, Germany

⁶Deutsches Zentrum für Luft- und Raumfahrt, Rutherfordstrasse 2, 12489 Berlin, Germany

[#]present address: Zivilingenieur für Technische Physik, Rheinallee 88, Gebäude 25, 55120 Mainz, Germany

*Corresponding author. E-mail: Andre.Schiele@esa.int

Abstract

This Paper describes the latest development status of the NANOKHOD micro-rover. The presented engineering model design is the culmination of a series of pre-developments that have taken place at ESA, industry and national research centers in the past decades.

The rover has undergone a major re-design to enable successful operations on the night-side surface of the planet Mercury. The extreme harsh operational environment is dictated by low temperatures approaching – 183 Degrees C, a regolith environment, and the lack of atmosphere. Several iterations in the design, paired with extensive testing of electrical and mechanical sub-systems were required to arrive at the presented design. For the first time, three scientific instrument front-ends are integrated into the Rover in engineering model quality. These instruments are an Alpha Proton X-ray Spectrometer (APXS) and a Mössbauer Spectrometer (MIMOS2) developed by Max-Planck Institute Mainz and Johannes Gutenberg-University of Mainz, respectively. A microscopic camera developed by DLR Berlin completes the suite of scientific instruments.

1. Introduction

Initially foreseen as a payload element of the Mercury Surface Element on the BepiColombo Mission, ESA initiated the ‘Mercury Robotic Payload’ (MRP) project to finalize the Nanokhod [2] [3] into a micro-rover engineering model. The goal set out by the activity was to establish a design that can withstand the

harsh environmental conditions on the night side of the planet Mercury.

The severe limitation of available mass and power for the BepiColombo surface element as a whole dictated a mass below 3.2 kg for the rover system. This includes payloads, electronics and Lander back-end. During the nominal mission duration of 7 days, the rover should not have consumed more electrical energy than 265 Wh and not have drawn more than 6 W peak power from the Lander at any time. The overall dimensions had to stay within an envelope of 240 x 165 x 65 mm, to make the Lander mission feasible. These stringent resource requirements prohibit the use of an autonomous rover and resulted in the preferred choice of a tethered rover.

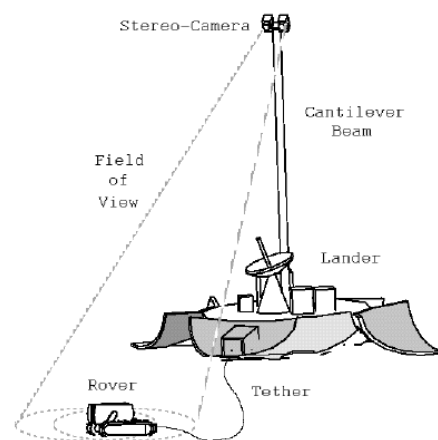


Fig. 1: Conceptual view of tethered Rover being deployed from a Lander.

The tether connection to the Lander unit provides power and data exchange. Once landed on the surface the vehicle is deployed from the landing craft onto the Hermian regolith surface (Fig. 1).

The analysis of the surface chemistry and mineralogy was one of the primary scientific objectives of the BepiColombo Mission with the initially planned lander element [1]. A primary goal of the rover was the support of the analysis of the element composition of surface materials and its content of iron bearing minerals. This would have been achieved by performing in-situ measurements of rocks and soil. The proposed micro-rover was to carry a geochemistry instrument package consisting of an Alpha-Proton X-ray Spectrometer (to measure chemical composition), a Mössbauer Spectrometer (to measure mineralogical composition), and a Camera to obtain images of surface structure and morphology in addition to surface reflectance spectroscopic data. The analysis of rock and soil samples up to a distance of about 50 m around the Lander was the target of the rover.

Despite the cancellation of the BepiColombo Landing element for cost reasons, in 2004 and thus, the loss of an immediate flight opportunity for NANOKHOD, the key objectives for the study were kept. This allowed us to gain important experience in the design, development and testing of miniaturized robotic vehicles for extreme environments. This can be of benefit to potential future missions with similar requirements. The goal of this paper is to present the re-design which was required to prepare the Nanokhod rover for application in extreme planetary environments, determined by temperatures approaching $-183\text{ }^{\circ}\text{C}$, a dusty regolith surface and the absence of atmosphere.

2. Method

2.1 Mechanical Design

With respect to prior developments that already aimed at improving robustness of some key mechanical sub-systems for a low temperature application [4], in this work, the entire Nanokhod design was iterated to eliminate all remaining shortcomings in the design. Fitting, gear, bearing and motor design, as well as pairing of materials was tailored appropriately to the extreme low temperature. Prior to incorporation into the design, low temperature functional tests have been performed to verify sub-system level performance.

In particular, a new sealing concept for the tracks has been introduced to improve seal performance in the regolith environment. The results overcome problems encountered during a previous study [5].

Furthermore, all gears have been changed to harmonic drives to improve payload cab positioning accuracy and track actuation robustness. Stepper motors along with their drive electronics have replaced conventional DC motors, to improve compatibility with vacuum. The structural design was improved to withstand the expected vibrations and shocks occurring during launch and landing.

The payload instruments have already flight heritage, and have been adapted to fit inside the restricted space of the payload-cab.

2.2 Electronic Design

For use on the night-side surface of planet Mercury, all electronics must be able to operate at cryogenic temperatures.

Because no off-the-shelf electronic parts exist for the required temperature range, a series of component tests had to be performed to aid the rover system design. Such tests were performed on all critical components and focused on ascertaining functionality and assessing parametric variation over the temperature range. Parts selected for the rover would not necessarily show ideal behavior but rather demonstrate a well predictable functionality. This allowed establishing design guidelines for compensating or reducing the effects of extreme low temperature on the components.

The following general design guidelines were applied:

Critical signals or signal processing should not be analogue, because of unpredictable gains and offsets over large temperature ranges.

If an analogue measurement is required, always measure differential.

Select active components to be MOS-type rather than BIP-type. Bipolar transistor gain for example reduces towards zero at temperatures around $-180\text{ }^{\circ}\text{C}$.

Reduce dependence on high accuracy RC timing circuits, wherever possible.

Radiation compatibility is furthermore important, with an expected total dose of about 22 kRad throughout the mission. Even though radiation tolerance is not required for the engineering model all critical components were chosen such that flight equivalent radiation hard components exist. Furthermore, the electronic architecture was designed such that transition to a radiation hard version would not require any major re-design.

2.3 Thermal Design

The general thermal concept of the rover is a passive one. The design goal was to retain as much

heat within the rover as possible, while avoiding local hot spots. These can easily occur for active components in vacuum. Therefore, following approach was followed in the design:

Heat conduction to the regolith via the tracks is minimized by design of a PTFE seal between structure and tracks.

Heat radiation to the outside is minimized using low emissivity finish, such as Alodine 1200 ($e = 0.12$).

All PCB's are mounted to the Rover structure via Al stand off's, to allow conduction and avoid local heating.

Thermistors measure the temperature of the main motor driver chips and other hot Power Supply components.

Some sensors contain thermistors to allow for calibration against temperature.

3. Results

3.1 Design Overview

The resulting MRP Rover design is shown in Fig. 2. Like its predecessors, the rover comprises of two tracked locomotion units, rigidly connected via a tether bridge.

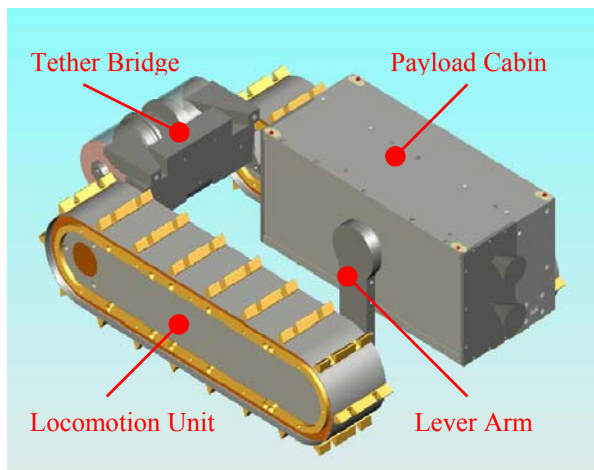


Fig. 2: The MRP Rover Model

The Payload cabin is attached to the two locomotion units via two lever arms. Two motor / gear assemblies, a lower and an upper one, actuate the left lever arm, providing two degrees of freedom for payload positioning. The right lever arm contains the cable harness to the payload cabin. The lever arms, locomotion units, payload cabin and tether unit are equipped with 9-pin micro NDDM connectors to greatly facilitate assembly and maintenance.

The entire stowed Nanokhod rover fits inside the volume specified with $240 \times 165 \times 65 \text{ mm}^3$. The total

system mass is 2.95 kg without margin, whereas the payload mass alone is 800 g, also without margin. Power consumed by the rover, as seen from the Lander, has an estimated peak at 5.7 W during locomotion. The rover will consume about 150 Wh of electrical energy from the Lander during the nominal mission duration of seven days. An estimate of telemetry volume for the baseline mission is about 4.6 Mbit, without science data. The science data volume is mainly driven by the camera images and their compression.

3.2 Rover Mechanical Design

Locomotion Units

The two locomotion units consist of two walls each, supporting the track foil around their circumference. The motor yokes (Fig. 3) connect both walls structurally. The track runs over two sprocket gears, out of which one is actuated per unit.

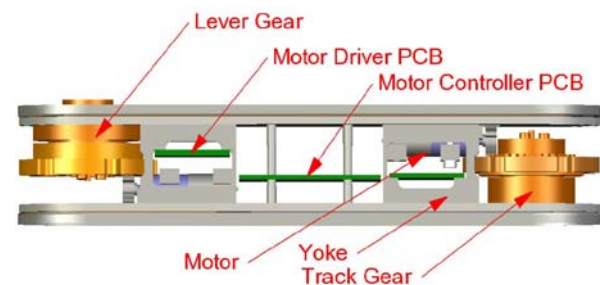


Fig. 3: Overview of left Locomotion Unit containing motor gear assemblies for track and lever actuation.

The right locomotion unit contains the motors and gears for forward and backward actuation of the right track. Furthermore it contains all PCB's for drive and control electronics of the motor, and the PCB containing the tether interface electronics, which is described later. The left locomotion unit (Fig. 3) contains the motor and gear unit for the actuation of the left track and additionally a motor and gear for actuation of the lower lever arm joint, which positions the payload cab. Furthermore all drive and control electronic PCB's are contained inside the locomotion unit housing.

The locomotion unit sealing is achieved at low temperature through a 0.25 mm thick PTFE seal, which is pre-loaded towards the Track-foil with a CuBe spring. The design was iterated several times and optimized for the extreme low-temperature case. Seal performance was analyzed by visual checks after cryogenic tests (Fig. 4). The seal and the spring are arranged such, that temperature related shrinkage of

the PTFE, the track or the spring does not negatively affect seal performance (Fig. 4, top left).

Seal contact pressure amounts to about 0.2 N/mm. This is sufficiently high to provide good sealing performance and sufficiently low to produce minimal friction. The total friction, per locomotion unit, sums to about 470 mNm at the gear output in room temperature. The friction decreases at low temperatures.

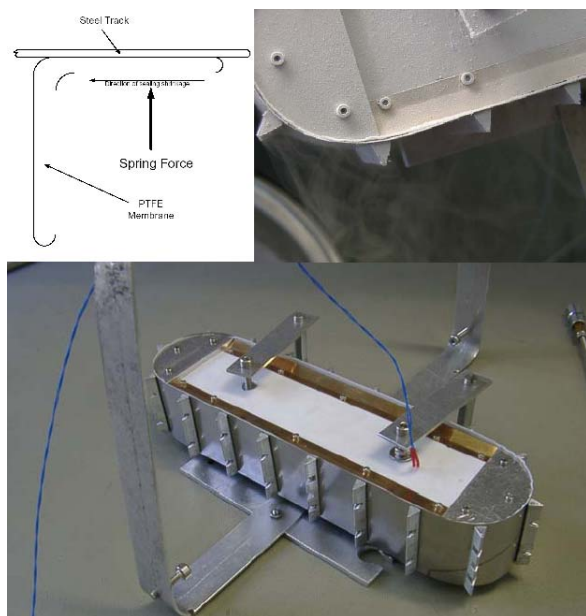


Fig. 4: Concept (top left) and prototype of track seal before (bottom) and after cryogenic test (top right).

Actuation

The locomotion design is similar for all drives. The drive-train design is strong enough to enable terrain gradeability of at least 20° on Mercury and Earth. Furthermore, the design allows the lever drives moving the Rover Chassis over the Payload Cabin, which is good for obstacle climbing capability. Locomotion velocity of the rover is about 3 m per hour. The chosen actuator is a decreased version of the AM1020 stepper motor, running constantly at 5000 rpm. All gear units of the rover incorporate HFUC series Harmonic Drives (HD), to reduce backlash to less than 5 arcmin and provide sufficient robustness against vibration and shock loads. For the track actuation, the motor output is coupled via a planetary gear head and a crown gear to the wave generator (WG) of a HFUC harmonic drive unit. While the flex-spline (FS) is fixed to the locomotion unit walls, the circular-spline (CS) is attached to the drive sprocket. The sprocket assembly is supported with bearings on the gear housing.

The concept of the lower lever drive is similar, with the difference that the flex-spline is connected directly to the lever, while the circular-spline is fixed on the locomotion unit walls. The passive sprocket that supports and guides the track is mounted around the circular-spline with bearings allowing it to run free. Sealings between the gear and the walls are provided by PTFE O-rings. The upper lever drive is arranged similar, with the circular-spline attached to the Payload Cabin structure. Furthermore, the pinion gear is inverted, to be more compact. A shaft for a rotational encoder is provided, from the wave-generator to the outside of the assembly (Fig. 5). The output torque of all motor-gear systems is about 3.2 Nm at the HD exit.

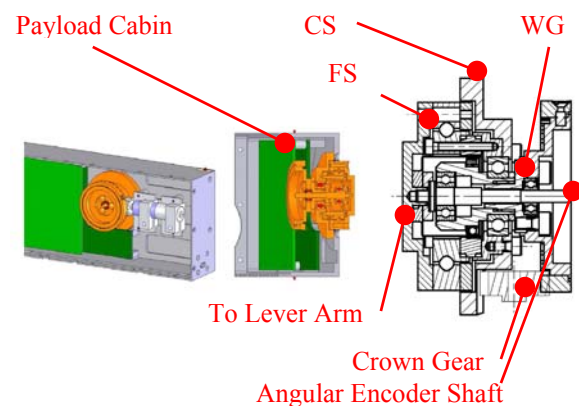


Fig. 5: Assembly of Drive Unit for upper lever Drive inside the Payload Cabin.

As the smallest possible size is desired for the HD gears, the fact of low number of revolution required during operation, plays an important role. It allows reducing the safety margins required for the gear, and opens the way to design the gear against ratcheting torque (Fig. 6).

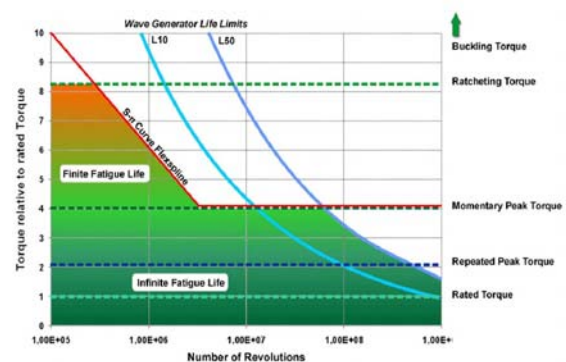


Fig. 6: Schematic of Torque and Wave Generator Limits for HD Gear versus number of revolutions. (Credits to Harmonic Drive AG, Germany)

A HFUC type gear was selected, as it provides a reduced length and generally higher ratcheting values towards the HDUC types.

The HFUC 05-08-2A-R-SP was chosen for all gear units. All contact surfaces, as well as the bearings are dry lubricated with Microseal 200-1, which is based on MoS₂ lubricant. The lubricant is according AMS 2526, which has passed all relevant ESA off-gassing tests. Thermal expansion characteristics were considered in the material selection of the gears. The selected parts consist of 15-5 PH, 17-4 PH, space qualified stainless steel and 440C for bearings.

Payload Cabin

The Payload Cabin of the rover (PLC) is designed to optimally integrate the geochemistry instrument package facility (GIPF), the central rover controller PCB and the motor driver / controller PCB's for the upper lever drive. Fig. 7 shows the arrangements of the science payload front-ends inside the PLC. All instruments are positioned axis symmetrically, such that they can be positioned on the same spot by rotating the upper lever drive only.

On each corner of the PLC LED's are situated, to support the Lander based visual localization system [6]. A ring containing micro-switches to detect contact with objects is mounted in front of the Mössbauer Spectrometer.

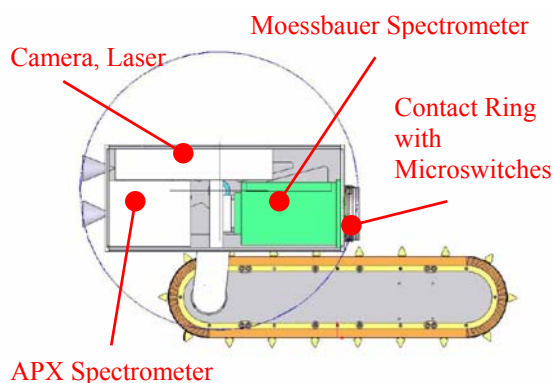


Fig. 7: Overview of GIPF Payload arrangement in Payload Cabin

Tether Unit

The Tether Unit has been slightly relocated, in order to increase ground clearance of the rover. Spring deployable tether guides ensure guidance of the unwinding tether and allow the rover to drive backward for at least his body length. The tether spools that contain each 50 m of RF litz, can easily be removed for inspection and testing. They are attached

via ball bearings to a central axis, to provide minimal unwinding resistance. Electrical contact between the unwinding tether and the rover is provided by gold-plated spring loaded slip-rings, that are sealed from the environment.

Lever Arms

The driven arm consists of two purely structural parts. Either end is connected to the flex-spline of the lever actuation units. The non-actuated arm passes the rover bus between the PLC and the right locomotion unit. A cable spiral at either end enables a 370° rotation of the lever. On the PLC side, the spiral is included in the arm itself, while the lower spiral is contained inside the Locomotion Unit to gain ground clearance through a smaller arm base diameter Fig. 8.

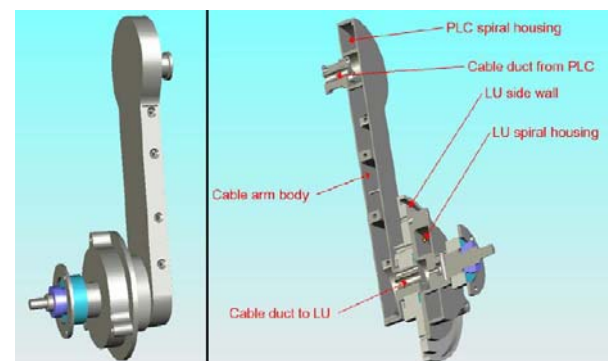


Fig. 8: Assembly view on right lever arm.

3.3 Rover Electrical Design

Tether Communications

Communication between the Lander and the Rover is performed via tether wires, which carry both, power (DC) and communication signals. The tether consists of two wires formed from 30 strands of 0.054 mm Cu-LS RF Litz. With respect to prior versions, the increased wire diameter reduces the overall resistance by over 25 %. The 50 m long wires are enamel insulated and are covered by a fine silk. One wire carries the power supply while the other one carries the return. Each wire is again split into two electrically separate bundles, to be able to carry differential communication signals. One wire is used for telecommand up-link, while the other wire is used for telemetry return. The differential signals are coupled to each wire by transformers (Fig. 9). The transceiver circuits convert the character coding generated by the logical units in the Rover or Lander into electrical signals that can be transmitted over the tether. Therefore, a differential driver followed by a pulse shaper is used in front of the Tx splitter.

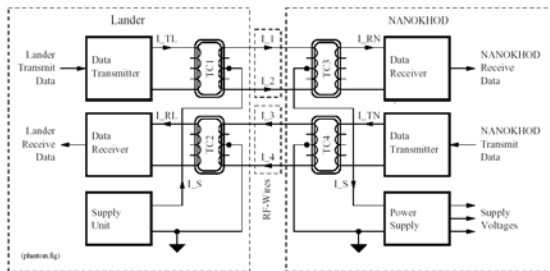


Fig. 9: Tether Data and Power Transmission Scheme

The Rx circuits are responsible to split the communications signals from the power supply. The splitting transformers are Arnold 0.4" MPP powder core, which have better permeability stability over the temperature range than usual ferrites. Even though the overall permeability is lower than for ferrites, it is better for establishing a constant working point for low power consumption over the entire temperature range. After EMI filtering, the Rx communications signals are fed to level detectors for conversion into logic level signals.

Power and Grounding

Power is directly supplied from the Lander power bus. For a 50 m tether, it is more efficient to pass a 28 V signal directly over the tether than an up-converted signal. The full galvanic isolation was abandoned. Due to the overall low power consumption of the rover, such an approach is allowable. However, it can only be followed, if the Lander bus is appropriately protected by active elements.

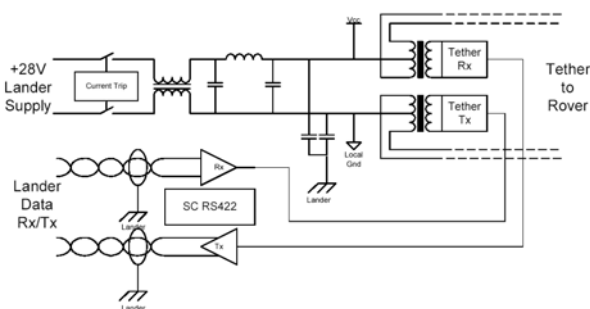


Fig. 10: Lander Side Power and Grounding Diagram.

Therefore, a solid-state current monitor protects both lines of the Lander bus (Fig. 10). After common mode and differential mode filtering, the power signal is passed to a pair of signal toroids to create two separate channels per wire, which is required for differential communications.

On the Rover side (Fig. 11), after separating power from communication signals and filtering with a

differential mode filter, the signal is passed to the power converter unit to produce regulated ± 5 V for further use. Furthermore a LM3488 controller switches the 28 V line for motor supply. The LM3488 provides PWM output and current limit and is rated down to -40 °C. Tests have shown that it is operational below -150 °C with a variation of operating frequency of less than 10 % at 1 MHz. The variation decreases at lower frequencies.

The presented solution has a power conversion efficiency of between 70 – 75 %, depending on the overall power level consumed. With full galvanic isolation to the Lander bus, efficiency would drop to 51 – 59 %, depending on the chosen transmission scheme over the tether.

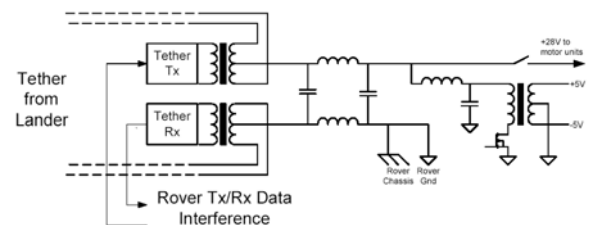


Fig. 11: Rover side Power and Grounding Diagram

Internal Bus

A new 9-wire serial bus system, using the I²C bus protocol for data exchange, has been incorporated into the Nanokhod. This drastically reduces the internal wiring with respect to prior versions. Several Nodes, each containing an I²C interface, act as functional blocks of the rover.

Rover nodes

The Rover Central Controller Node and the Tether Unit Node are core systems and remain always powered. The aim of the on-rover controller is to be a central control unit for rover and integrated payloads. However, integration of Payload back-end electronics is still to be performed in a future activity, which is why the central controller structure can still change at a later stage. In a flight version, an FPGA with implemented IP core, e.g. an 80C51 type processor, would be selected. For the engineering model, an 8-bit micro controller, which has similar capabilities, is chosen, but only functionality that can also be implemented in a FPGA is used. The selected device is a Philips P87C552. Even though the device has its own RAM and EPROM, external RAM / EEPROM / PROM units, are used, which are representative for the flight units. The internal ADC was furthermore not used but replaced by an external one. This was done to establish a flight equivalent design.

Three additional nodes are motor controller nodes. Their design is again a generic one. The nodes are implemented in the right and left track, as well as in the Payload Cab. These nodes may be powered down, when not in use. Their state is controlled by the 28 V line, that also supplies the power to the motors. If the 28 V are not present, the node switches off. Power-cycling the 28 V line can reset a disabled node. Each of these Nodes can interface to up to 2 motor driver boards that contain the current controllers for the motors. Furthermore, the generic motor controller nodes are responsible for collecting housekeeping data of the sensors distributed around the rover. Their design is illustrated in Fig. 12. Because all of these nodes have independent oscillators, time synchronization of their oscillator frequencies is performed. The synchronization is achieved by the general broadcast message facility of the I²C.

In a flight design, common functionality of all nodes would be implemented in a mixed signal or digital ASIC. This would result in a radiation hard design, with good immunity to Single Event Upsets.

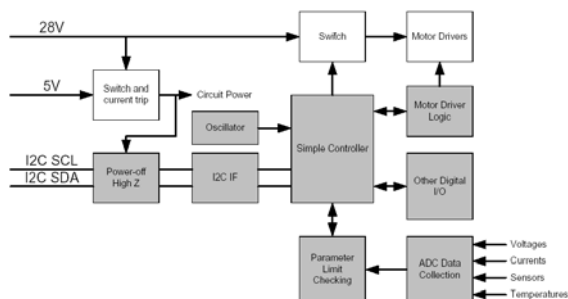


Fig. 12: Node design of Motor Drive Node (Grey boxes show functionality to be implemented into an ASIC)

Considered processes are the MG2RT (0.5 μm) from Amtel, or the Aeroflex CRH (0.25 μm) processes. For this project, the ASIC functionality is mimicked by a Motorola 8-bit microprocessor. Again, only representative functionality of the microprocessor is used. The ADC is an external one, and is simulated by an AD7888. This 12-bit ADC is functional at -180°C . It shows a deviation of about 5 mV at -80°C , and about 3 mV at -150°C , which corresponds to a maximum of 8 LSB and 5 LSB at low temperatures. For radiation compatibility an Intersil HS0548RH together with an AD574 could be used to replace the engineering model design.

Motor Drivers

The motor driver boards are located next to the motors to provide some EMC separation from the node board. The motors always operate at constant speed, in a current control mode. The control circuitry is implemented using a STC L6207 motor controller. The IC provides current control and motor switching in a single CMOS package. With a chopping frequency of 43 kHz a step speed of 1.6 kHz (~ 5000 rpm) is achieved in the motor. An increase of required current was detected during cryogenic tests.

Sensors

Sensors of the Rover are acquired via the 8 channel ADC's on each rover node and provided to the central controller.

To measure the angles of the Payload Cab, endless rotational potentiometers PIHER N-15 are used. They are preferred over optical encoders, due to their lower power consumption and better suitability in dusty environments. The angle is acquired via differential measurements to compensate for temperature drift in carbon film and voltage supply.

The rover can measure the gravity vector with three accelerometers that are placed in an orthogonal set inside the locomotion units. The ADXL203 has shown repeatable output characteristics during cold temperature tests, however, needing some local heating or recalibration with calibration tables.

Contact sensors for detecting a docked Payload Cabin to a target are mechanical switches (ITT KSR Series), which have proven to function properly in cryogenic temperatures only, once their membrane is exchanged with a thin PTFE membrane. They are more lightweight and compact than any other possible contact sensors.

Furthermore, voltages currents and temperatures of the rover electronics are monitored and converted by the 8 channel ADC's on each node.

3.4 Rover Payload

For the first time, the Nanokhod integrates the front-ends of 3 scientific instruments and a laser stripe sensor into the Payload Cabin.

Two of the instruments have flight heritage, while one, the camera is a new development. However, all three GIPF front-ends are built in engineering model quality and will undergo extensive environmental and functional testing in the future. The instrument back-ends are still external to the rover and will be integrated and miniaturized into a Common Subsystem in a following development step. In the current stage, the Rover Controller reserves allocations for the Common Subsystem.

MIMOS2 - Mössbauer Spectrometer

The purpose of the MIMOS instrument is to identify iron bearing minerals.

The Mössbauer Spectrometer is developed by the Institute of Inorganic and Analytic Chemistry at the University of Mainz. The instrument has flight heritage, being part of the Beagle2 Lander [7] and being scientific payload on the Spirit and Opportunity Rovers of the MER mission [8]. The instrument has undergone some minor changes in mechanical design, in order to optimally integrate into the Rover Payload Cabin (Fig. 13).

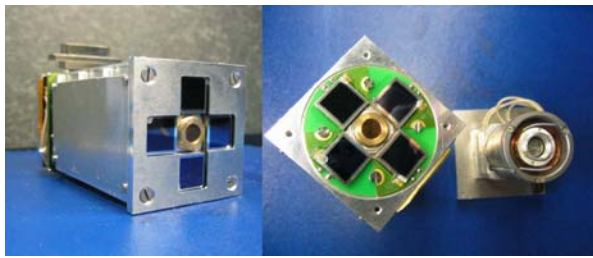


Fig. 13: GIPF front-end of the Mössbauer Spectrometer as adapted for the Payload Cabin of the Nanokhod. Assembled view (left) and MB drive disassembled from detectors (right). Developed by Univ. of Mainz.

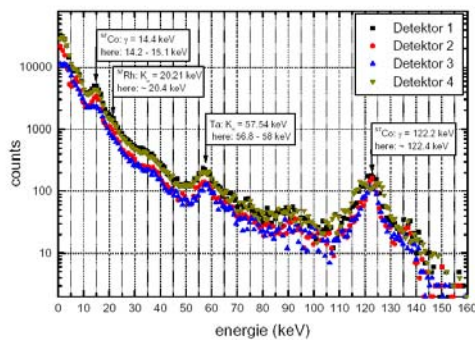


Fig. 14: First Energy Spectrum measured with new GIPF Sensor head. For comparison the literature values of some materials of the source (^{57}Co in Rhodiummatrix) are shown.

Furthermore, to improve radiation shielding with respect to prior designs, the outer Mössbauer (MB) drive tube was manufactured entirely in tantalum.

For a better handling, each detector of the new Sensor-head can be changed without dismantling them all.

First measurements of the GIPF front-end, without optimized setting of the discriminator thresholds, show the principal readiness of this sensor-head (Fig. 14).

The overall dimensions of the Sensor-head are rectangular, with a cross section of 41 x 41 mm and a length of 81 mm. The overall mass of the Sensor-head for GIPF is 300 g.

APXS - Alpha-Particle X-ray Spectrometer

The purpose of the Alpha-Particle X-ray Spectrometer is the determination of the elemental chemical composition of geological samples.

This instrument has a long heritage as a flight instrument for space missions. The APXS was, among others, part of Pathfinder, Rosetta and the MER missions. On MER, the spectrometer is attached as scientific payload to the Spirit and Opportunity Rovers.

With respect to the MER design of the instrument [9], some changes have been performed to the sensor-head to allow integration into the Nanokhod Rover. First of all, removing the cylindrical external casing, the protective door mechanism and the alpha detector system (including the PCB's with the alpha-detector preamplifiers) reduced the size of the instrument. Due to a greatly improved x-ray detector system, the alpha channels become of extremely little value and will, in fact, be omitted in all future instrument versions. The protective door mechanism has proven not to be required on Mars. Changes of the sensor-head are illustrated in Fig. 15 and Fig. 16.

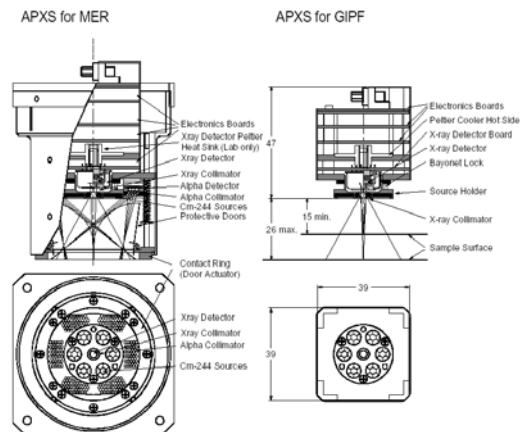


Fig. 15: APX Sensor-head comparison between MER and GIPF design.

Added benefit of the mechanical rearrangement was the increase of sensitivity of about 2.5 times (Fig. 17), which resulted from a reduced working distance of 15 mm, instead of the earlier 26 mm. The resulting instrument front-end has a rectangular external envelope. The cross section is 40 x 40 mm, while the length of the sensor-head is 47 mm. The mass of the

sensor-head alone is 85 g. The sources have a mass of 30 g.

Regarding the instrument back-end electronics, the traditional analogue electronics plus microcontroller have been replaced with a commercial digital signal processor, the μ DXP provided by X-ray Instrumentation Associates, Newark, CA. The porting into complete digital domain is a first important step to enable miniaturization of the complete instrument electronics into the Nanokhod Rover. The reason for choosing the μ DXP is the fact that all filter algorithms are implemented in hard-wired logic on a Xilinx FPGA. This will allow in a next step to transfer the key technology into a space qualified radiation-hard FPGA.

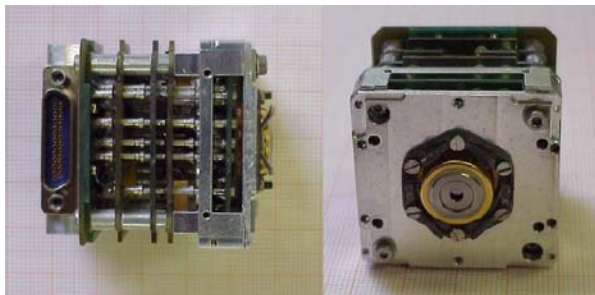


Fig. 16: The new APXS Front-end developed for the Nanokhod Payload Cabin (without sources) by MPICH in Mainz. Side view (left) and front view (right).

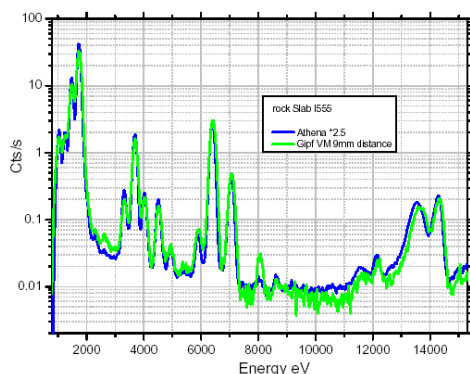


Fig. 17: Comparison of response for different working distances (Sample I555, andesitic basalt): APXS for MER – 26 mm x 2.5, APXS for GIPF – 17 mm.

Interference between MIMOS and APXS

Measurements have shown that due to the close geometry of the Payload Cabin, the ^{57}Co sources, in particular the calibration source, of the Mössbauer Spectrometer significantly increases the background of the X-ray APXS spectra. Measured background from an 80 mCi ^{57}Co source are shown with different

shielding set-ups in Fig. 18. The placement of the source as well as the strength of the source was representative for the instruments and their accommodation in the payload cabin.

In order to achieve meaningful measurements with the APXS near the MIMOS, a 10 mm Densimed (porous W filled with alloy of Ni, Fe or Cu, density $\sim 17 \text{ g/m}^3$) shield has to be additionally implemented between the instruments. The shield must be implemented near the source, close to the MB drive.

The influence of APXS radioactive sources to Mössbauer Spectra is negligible.

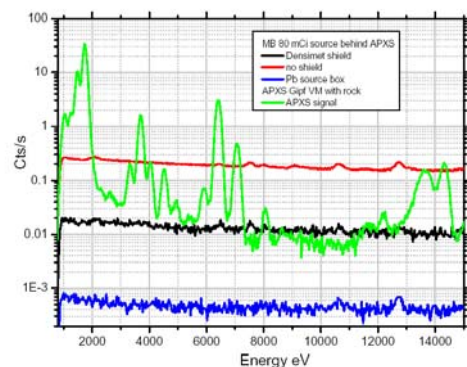


Fig. 18: Background in APXS X-ray spectra due to MIMOS source with different shielding: no shield (red), 10 mm Densimed shield (black), enclosure of MIMOS source in 10 mm lead container (blue).

MIROCAM - Microscopic Camera

The goal of the MIROCAM is to provide close-up images of the same field of view as covered by the MIMOS and APXS. The Institute of Planetary Research, of the German Aerospace Agency in Berlin, has newly developed the MIROCAM under ESA contract.

The complete Camera System is integrated into a very small package. The cross section is 20 x 40 mm, with a length of 100 mm. A picture of an early prototype is shown in Fig. 19.

Considering the uncertainty in the distance estimate from the lens to the sample surface, as well as the surface roughness of the samples, an auto-focus system was developed for the MIROCAM. Moreover, additionally to close-up imaging, the camera can change the focus to infinity in order to support navigation of the rover. The opto-mechanical system (Fig. 20) is based on an ARSAPE AM1020 stepper motor, in combination with a MHD10-160-H harmonic drive gear – developed by Micromotion GmbH. An excenter converts the rotary output onto a linear ‘Schneeberger’ table that carries the Lens system.

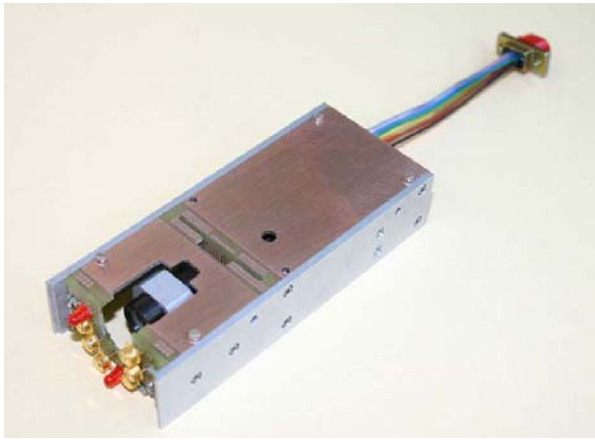


Fig. 19: Assembly view of MIROCAM camera developed by DLR Berlin.



Fig. 20: MIROCAM Opto-mechanical system.

Four pairs of Red, Green, Blue and Infrared LED's are arranged around the camera aperture, for illumination of the target surface. The LED's are switched by Vishay Si3865 power switches.

The image sensor of the first prototype is the LM9637, 648(h) x 488(v) monochrome active pixel sensor. It is placed behind a modified lens from 'Thales Optic' with focal length of 8.3 mm.



Fig. 21: Infinity and Close-up pictures taken by MIROCAM

The electronics of the Camera are based on a Xilinx Spartan 2 FPGA (XC2S100) that includes all control

electronics for the APS Sensor, the LED illumination and the focus control. An additional driver component for the stepper motor is the L293DNE integrated circuit. The camera can be fully controlled by an I²C serial interface from the Common Subsystem. Demonstration pictures are shown for infinity and close-up modes in Fig. 21.

Laser Stripe Generator

The purpose of an integrated laser line generator is to allow implementation of simple navigation functions into the Nanokhod. A simple laser line extraction algorithm will be used on the MIROCAM images for orientation and distance detection of obstacles such as rocks or trenches. This information can be used for approaching and docking of the payload cabin to scientifically interesting targets.

A laser plane is projected horizontally out of the Payload cabin with a fan angle of 14°. A laser diode (Stocker Yale Mini Laser) with a non-gaussian line projection optic produces a uniform intensity line. The accommodation inside the Payload cabin was optimized to increase the maximum and minimum distance at which an obstacle can be recognized with the given geometry (Fig. 22). With the given position inside the payload cabin, objects can be detected in distances from 105 – 630 mm.

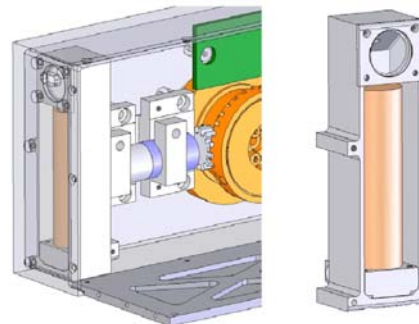


Fig. 22: Laser Stripe Generator accommodation inside Payload Cabin.

The Laser Diode functions properly at cryogenic temperature, and analysis has shown that a laser source of 1 mW is sufficient for applying the navigation computations.

Common Sub-system

The development of the Common Subsystem is still at an early stage. The integration of the instrument back-ends into one system is the subject of a dedicated study. The goal for that 'GIPF Common Subsystem' is to connect all three instruments, the MIMOS, APXS

and MIROCAM to one single communication line, handle their data and commands and distribute and switch their power. Furthermore, large portions of the instruments digital electronics will be joined together. This is expected feasible, as all designs can make use of similar FPGA technology. The common sub-system will ideally be integrated with the Rover Controller, for which, at this stage, a set of rather generic resources are allocated.

3.5 Rover Navigation

The Navigation concept of the Nanokhod is similar as in previous versions, with some extensions. Navigation is still mainly Lander based. Stereo Cameras recognize LED's attached to the rover (Fig. 23) to determine its position and orientation in the terrain [6] [10]. However, in the current Rover, tilt sensors are integrated, which allow to continuously check for hazards such as tipping over due to very steep slopes.

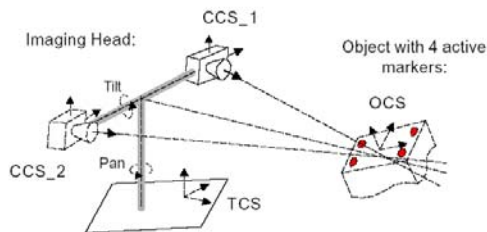


Fig. 23: Schematic Navigation Concept of Nanokhod. Imaging Head attached to Lander base will recognize active markers attached to Rover Payload Cabin.

Furthermore, the inclusion of the laser plane generator allows implementing some reduced local autonomy in the rover itself, which furthermore unloads the Lander computer. The structured light generation is used in the following way.

A light source projects a known pattern of light into the scene. Terrain slope or object / obstacle detection is done by performing a series of MIROCAM measurements of the projected single horizontal light-beam at different but known payload cabin angles with respect to the terrain. Based on rotational information provided by the Payload Cabin sensors, the camera acquisitions are assembled into a multi line picture. Onto this picture, feature extraction algorithms are applied. Fig. 24 illustrates the concept, how three

different line reflections assembled in one camera picture indicate the presence of a potential obstacle.

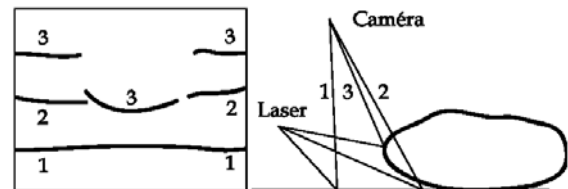


Fig. 24: Use of structured light to extract environment information from a sequence of 3 images.

The Rover will be able to send this information back to the Lander, to request an appropriate reaction or to execute some locally implemented routines. This way, constant monitoring by Lander stereo imagery can be reduced, which will save energy for the mission.

3.6 Rover Energy

Energy required to perform essential tasks is shown in Fig. 25. All values are calculated using the baseline mission definition for instrument measurement durations. A 'segment' corresponds to 40 cm drive of the rover, whereas a 'Sub-segment' describes a 90° rotation.

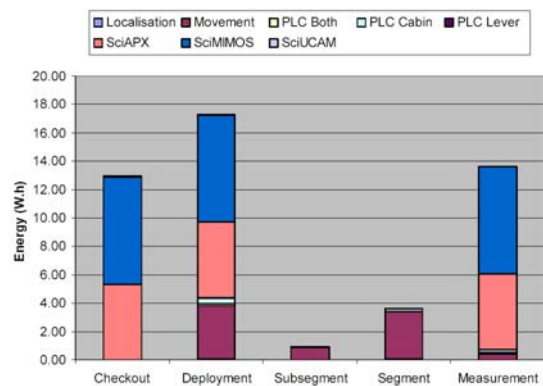


Fig. 25: Energy required by the Rover during several mission steps.

4. Discussion and Conclusions

With respect to prior Nanokhod versions, this paper introduces an engineering model design, which is optimized for application on the night-side surface of planet Mercury. The presented design has been optimized to withstand cryogenic temperatures approaching those of open space, vacuum and dusty

regolith soil. While the Nanokhod Engineering Model is still under construction at the time of writing, extensive testing has already been performed on key sub-systems under cryogenic conditions. This strengthens the confidence in a successful implementation of the design.

In particular, a new sealing design has been developed and successfully tested. Furthermore, a new, more efficient power transmission scheme has been designed. It is optimized for the given tether length and the overall low power consumption of the rover. A serial bus within the rover, serves several nodes that fulfill all functions related to the rover operations. The electronic architecture is chosen such that radiation-hard space qualified flight components can be used in the next instance, without a required major re-design. The drive-train of the rover has been re-designed to be able to overcome obstacles of 0.1 m height and provide terrain gradeability of over 20°. Furthermore stiffness of the Payload Cabin has been improved through replacing the worm gears with Harmonic Drives. This has also led to much higher positioning accuracies with respect to previous designs. In general, all requirements posed by using BepiColombo as a reference mission are fully met by the design.

Furthermore, for the first time, front-ends of three scientific instruments, the APXS, MIMOS2 and MIROCAM are fully integrated into the payload cabin at engineering model quality. The common sub-system to fully integrate the current instrument back-ends into the rover is still under development together with ESA. Experiments have successfully demonstrated the feasibility of using the APXS and MIMOS2 together, in tight integration. This might open the way to a dedicated geochemical instrument package facility that can be used even independently from the rover, eventually delivered as a 'plug-and-play' instrument.

It is envisaged to perform extensive testing in cryogenic temperatures with the engineering model. Tests will be performed in vacuum and dust environment at the same time. Vibration testing of the entire integrated Rover will take place in 2005.

Furthermore, tests will be carried out with the GIPF science package, to analyze in more detail their performance.

References

- [1] "BepiColombo, An Interdisciplinary Cornerstone Mission to the Planet Mercury", System and Technology Study Report, ESA-SCI(2000)1, April 2000
- [2] R. Rieder et al., "Nanokhod: A miniature instrument deployment device with instrumentation for chemical, mineralogical and geological analysis of planetary surfaces, for use in connection with fixed planetary surface stations", Lunar and Planetary Institute, LPS XXVI, 1995, pp. 1161 – 1162
- [3] R. Bertrand, R. Rieder, M. v. Winnendael, "European Tracked Micro-rover for planetary surface exploration", Proceedings of ASTRA Workshop, ESA, 1998
- [4] R. Bertrand, M. v. Winnendael, "Microrover Design for Extreme Environments", Geophysical Research Abstracts, Vol. 5, European Geophysical Society, 05724, 2003
- [5] R. Bertrand, J. Dacolmo, S. Klinkner, "RTPE: Robotic Technology for Planetary Exploration", ESA, Final Report, RTPE-54-10, 2003
- [6] M. Vergauwen, M. Pollefeys, L. van den Gol, "A stereo vision system for support of planetary surface exploration", International Conference for Computer Vision Systems (ICVS), Canada, 2001, pp. 298 – 312
- [7] C. T. Pillinger, "The guide to Beagle 2", C.T. Pillinger & Faber and Faber, 2003
- [8] G. Klingelhöfer, R.V. Morris, B. Bernhardt, D. Rodionov, P.A. de Souza jr., S.W. Squires, J. Foh, E. Kankeleit, U. Bonnes, R. Gellert, C. Schröder, S. Linkin, E. Evlanov, B. Zubkov, O. Prilutski, "Athena MIMOS II Mössbauer spectrometer investigation", Journal of Geophysical Research, Vol. 108 (E12), 2003, pp. 8-1 – 8-18
- [9] Rieder, R.; Gellert, R.; Brückner, J.; Klingelhöfer, G.; Dreibus, G.; Yen, A.; "The new Athena alpha particle X-ray spectrometer for the Mars Exploration Rovers", Journal of Geophysical Research, Vol. 108 (E12), 2003, pp. 7-1 – 7-13
- [10] B-M. Steinmetz, K. Arbter, B. Brunner, K. Landzettel, "Autonomous Vision Based Navigation of the Nanokhod Rover", iSAIRAS No. 6, 2001, Montreal, Canada